Journal of the Earth and Space Physics, Vol. 43, No. 4, Winter 2018, P. 27-45

Inversion of Gravity Data by Constrained Nonlinear Optimization based on nonlinear Programming Techniques for Mapping Bedrock Topography

Karimiara, A.[1], Mirzaei, M.[2*] and Babaei, M.[3]

1. M.Sc. in Geophysics, Department of Geophysics, Hamedan Branch, Islamic Azad University, Hamedan, Iran
2. Associate Professor, Department of Physics, Faculty of science, Arak University, Iran
3. Assistant Professor, Department of physics, Tuyserkan Branch, Islamic Azad University, Tuyserkan, Iran

(Received: 5 Nov 2016, Accepted: 24 Oct 2017)

Abstract

A constrained nonlinear optimization method based on nonlinear programming techniques has been applied to map geometry of bedrock of sedimentary basins by inversion of gravity anomaly data. In the inversion, the applying model is a 2-D model that is composed of a set of juxtaposed prisms whose lower depths have been considered as unknown model parameters. The applied inversion method is a nonlinear one, which minimizes the objective functions by definition of different objective functions and an initial simple model to improve the initial model parameters. In this study, for different cases, sufficient objective functions are defined based on the condition which is encountered in the inverse problem. To control the under- determinacy part of the inverse problem and to prevent unreasonable instability in the resultant model, damping terms are added to the objective function. The act of synthetic inversion for different cases of parameterization has been examined and the results are analyzed. The results have almost depicted the recovery of the model and also fitting of the original and model response data. In addition, the method has been used to invert real gravity data in Aman Abad area. From the inversion results, depths of the basin, features like fractures and uplift in bedrock, along specific profiles have been determined. Thicker parts of sediments in the basin along the profiles have also been recognized, which have the potential for exploring drinking water in this area.

Keywords: Optimization, Objective function, Geometry of bedrock, Inversion, Constrains, Gravity data.

1. Introduction

To map the sediment thickness and bedrock topography, there have been various methods in recent years by which we can find many applications for these types of mapping in subsurface geological investigation such as: geotectonic, modeling groundwater flow, exploring petroleum, studying ice stream flow and modeling ground motion amplification during an earthquake in a sedimentary basin. It is known for certain that the basis of understanding of a ground water system in a valley or determining a major faulting system depends on sediment thickness and bedrock topography (Annecchione et al., 2001; Schaefer, 1983).

If interface intersects any vertical line only once (Smith, 1961) and the gravity anomaly is known to exist in a continuous way with infinite precision, mapping the depth to an interface, separating the two homogeneous media will be considered to a nonlinear problem with a unique solution. The knowledge of the discontinuous relief of a sedimentary basin could also lead to locating oil structural traps, to be of combination with the discontinuity (Silva et al., 2010). Because of the higher density (higher seismic velocity) of bedrocks than that of sedimental, alluvial, or volcanic deposits, seismic waves can be trapped and thus amplified, resulting in disastrously large ground motion and extended earthquake duration. The Knowledge of a subglacial sediment can be efficiently used to understand the dynamic evolvement of the ice streams in Polar Regions (Bell et al., 1999; Studinger et al., 2001).

In practice, these last conditions are never fulfilled making the solutions become unstable. Therefore, there are methods designed to solve this problem, which introduce an a priori information to stabilize the solutions (Burkhard and Jackson, 1976; Pedersen, 1977; Richardson and MacInnes,

*Corresponding author: m-mirzaei@araku.ac.ir

1989). Stabilizing the problem condition can also be accomplished by limiting the parameter corrections at each iteration, using, for example, a parameter covariance matrix (Burkhard and Jackson, 1976; Richardson and MacInnes, 1989) or abandoning eigenvalues smaller than a threshold one in a generalized inverse approach (Pedersen, 1977).

The clear former information required by these methods can be a good guess for the thicknesses of the upper medium and the knowledge of the density contrast between the media.

Oldenburg and Pratt (2002) developed an iterative method based on Parker's expansion of the gravity anomaly into a power series of the function representing the interface in the wave number domain (Parker, 1973). Parker's formula was represented in a noniterative inversion by Guspi (1993), expressing it as a power series expansion in the reciprocal of the density contrast.

In Granser's method, the kernel of the nonlinear integral equation relating the gravity anomaly to the interface relief is expanded in Taylor's series with the coefficients of the inverse series obtained from the coefficients of the original series (Granser, 1987). If the low-pass filter is applied to the observed anomaly, these methods stabilize the solutions, with a cutoff frequency designed to guarantee the convergence of the series. The lower cut-off frequency and the low order of the expansion, result in a stable inversion, the more stable solutions and the smoother estimated interface. The only clear former information necessary to be taken into account is the density contrast between the two media and the interface average depth. Successive approximations of the interface were obtained by computing the residual associated relief between the observed and the computed anomaly using the current approximation for the interface at each iteration. Added to the previous approximation is the residual topography (Courtillot et al., 1974; Pilkington, 2006).

In these methods, at each iteration either an integral equation (Courtillot et al., 1974) or a matrix equation (Pilkington and Crossley, 1986) is solved, being equivalent to continued observed anomaly to some level below the surface. The stabilizing procedure is therefore reduced, to stabilize the downward continuation procedure, in the matrix formulation of Pilkington and Crossley.

Two inversion methods can be used to determine the bedrock topography and probable discontinuities. Inversions can be performed manually by adjusting the geologic model manually, or automatically using an optimization algorithm. Barbosa, Silva, Oldenburg and Pratt did review different methods (Barbosa et al., 1999; Oldenburg and Pratt, 2002).

Fourier method was the basis of several algorithms using Parker's formula (Li, 2010; Parker, 1973; Pilkington, 2006). The implementations take advantage of the rapid forward calculations of gridded data via the Fast Fourier Transform (FFT) while forming the backbone of several commercial software products. Methods based on Parker's formula (computing the gravity effect of an arbitrary interface separating two homogeneous media) that stabilize the solutions either by applying a low-pass filter to the data or by using a damping parameter, implicitly introduce an a priori information in which the interface is smooth. The lower the cutoff frequency or the larger the damping parameter, the smoother the computed interface is.

Gravity inversion corresponds to a linear (density unknown) or nonlinear (geometry unknown) inverse problem depending on the model parameters. Among the nonlinear techniques, inversion of basement relief of sedimentary basins is an important application which remains to be considered. A common way to approach this problem consists of discretizing the basin using polygons (or other geometries), and iteratively solving the nonlinear inverse problem by local or global optimization. Nevertheless, this kind of approach is highly dependent on the prior information used and lacks a correct solution appraisal (nonlinear uncertainty analysis). When the geometry of the bodies is unknown, there will be made some assumptions about the values of the corresponding densities. Among the nonlinear techniques, the inversion of

basement relief of a sedimentary basin is a relatively common task (Barbosa et al., 1999; Blakely, 1996; Chakravarthi and Sundararajan, 2007; Zhou, 2013).
Nonlinear gravity inversion of basement relief in sedimentary basins can be considered as a 2D or 3D problem depending on the model conceptualization. The 2D case is seen to be very common, consisting of the inversion of one or different profiles across the basin, generally with its maximum depth.
A nonlinear optimization is the classical way to tackle this problem, where the unknowns are the depth of the basement at certain locations, or the depth and some additional parameters to take into account the density variations of the sediments with position. As inverse problems are being more complicated in the real world, it is a need to use better optimization algorithms. Almost in all optimization problems, the goal is to find minimum or maximum of an objective function. Today, different researchers in the field of computer science, mathematics and physics seek to invent new methods, make more compatibility and harmony in inversion method. In this regard, getting solutions of the inverse problems can be achieved by optimizing methods where an objective function, including parameters that describe the model in the nature, can be defined. In using optimizing methods, the parameters will be estimated when an objective function can be minimized.
This paper has applied an inversion technique in gravity and for a problem, by defining different objective functions, including parameters which describe the models. In this work, a constrained nonlinear optimization method for gravity data inversion has been used where linear or nonlinear constraints can be considered to model parameters.
In this study, the subsurface is also divided into rectangular prisms while iterative nonlinear optimization technique is used to estimate the thickness of elementary prisms that approximate the sedimentary basin geometry.

2. Inversion Methodology

2.1. Forward Model

Forward model is considered for the inversion is a 2-D model. The 2-D model in x-z plane can be divided into M rectangular prisms which approximate a sedimentary basin. Density contrast between sedimentary and its bedrock will be considered constant. Effect of vertical component of gravity (g) of one of these prisms in one observation point with position (x_0, y_0), on the surface earth, can be calculated by the following relation (Plouff, 1966):

$$g\left(x_0, z_0\right) = K \rho \int_x \int_z \nabla_z \log \frac{1}{\left| \mathbf{r} - \mathbf{r_0} \right|} dx\, dz \quad (1)$$

where K is the universal constant of gravitation, ρ is density contrast, $\mathbf{r_0}$ is vector distance from the observed point to origin and **r** is vector distance from the origin to a point of anomalous body (prism). After integration, the gravity effect of one of the prisms at one observation point is shown below (Plouff, 1966):

$$g = K\rho \left\{ \begin{array}{l} x_2 \log \dfrac{x_2^2 + z_2^2}{x_2^2 + z_1^2} + \\ 2z_2 \left(\tan^{-1} \dfrac{x_2}{z_2} - \tan^{-1} \dfrac{x_1}{z_2} \right) - \\ x_1 \log \dfrac{x_1^2 + z_2^2}{x_1^2 + z_1^2} - \\ 2z_1 \left(\tan^{-1} \dfrac{x_2}{z_1} - \tan^{-1} \dfrac{x_1}{z_1} \right) \end{array} \right\} \quad (2)$$

where x_1, x_2, z_1, z_2 are the bounds of prism. Usually, n layers and n-1 interfaces are considered. Each layer includes M prisms that lower bound will estimate interface between the layers. Each layer and each prism number is shown by index i and j respectively. Therefore, the effect of these M prisms in an observation point can be estimated by adding the gravity effect of all prisms. Considering that the density contrasts in one layer for all prisms are equal, the following relation is arranged for programming purposes from the above equation:

$$
g=K\left\{\sum_{i=1}^{n}\sum_{j=1}^{m}\left(\rho_i-\rho_{i+1}\right)\left(\begin{array}{l} x_{2ij}\log\dfrac{x_{2ij}^{2}+z_{2ij}^{2}}{x_{2ij}^{2}+z_{1ij}^{2}}+ \\ 2z_{2ij}\left(\tan^{-1}\dfrac{x_{2ij}}{z_{2ij}}-\tan^{-1}\dfrac{x_{1ij}}{z_{2ij}}\right)- \\ x_{1ij}\log\dfrac{x_{1ij}^{2}+z_{2ij}^{2}}{x_{1ij}^{2}+z_{1ij}^{2}} \end{array}\right)- \right. \\ \left. 2z_{1ij}\left(\tan^{-1}\dfrac{x_{2ij}}{z_{1ij}}-\tan^{-1}\dfrac{x_{1ij}}{z_{1ij}}\right)\right\} \tag{3}
$$

where g is the gravity effect of all prisms in a measured point. In other words, the gravity effect of these prisms in each layer, with a constant density for a layer that can approximate the gravity effect of a sedimentary basin. For a two layers model, the value of **n** is set to 2.

2.2. Constrained Nonlinear Optimization Method

2.2.1. Optimization Theory Overview

Optimization techniques are used to find a set of design parameters, $\mathbf{x} = [x_1, x_2, ..., x_n]$ that can, in some way, be defined as optimal. In a simple case, this might be the minimization or maximization of a characteristic system that is dependent on $\mathbf{x}$. In a more advanced formulation, the objective function, $f(\mathbf{x})$, to be minimized or maximized, might be subject to constraints in the form of equality constraints, $G_i(\mathbf{x}) = 0$ ($i = 1,...,m_e$); inequality constraints, $G_i(\mathbf{x}) \leq 0$ ($i = m_e + 1,...,m$); and/or parameter bounds, $\mathbf{x}_l$, $\mathbf{x}_u$ (lower and upper bound).

A General Problem (GP) description is stated as:

$$\mathbf{min_x\, f(x)} \tag{4}$$

Subject to

$$\mathbf{G_i(x) = 0, i = 1, \dots, m_e,} \tag{5}$$

$$\mathbf{G_i(x) \leq 0, i = m_e + 1, \dots, m,} \tag{6}$$

$$\mathbf{x_l} < x < \mathbf{x_u}. \tag{7}$$

where x is parameters vector with length n, f(x) is the objective function, which returns a scalar value, and the vector function G(x) which returns a vector of length m containing values of the equality and inequality constraints evaluated at x. An efficient and accurate solution to this problem depends not only on the size of the problem in terms of the number of constraints and design variables, but also on characteristics of the objective function and constraints. When both the objective function and the constraints are linear functions of the design variable, the problem is known as a Linear Programming (LP) problem. Quadratic Programming (QP) concerns the minimization or maximization of a quadratic objective function that is linearly constrained. For both the LP and QP problems, reliable solution procedures are readily available. More difficult to solve is the Nonlinear Programming (NP) problem in which the objective function and constraints can be nonlinear functions of the design variables. A solution of the NP problem generally requires an iterative procedure to establish a direction of search at major iteration. This is usually achieved by the solution of an LP, a QP, or an unconstrained subproblem.

2.2.2. Active Set Algorithm

In constrained optimization, the general aim is to transform the problem into an easier subproblem that can then be solved and used as the basis of an iterative process. Solutions of this problem have focused on the solution of the Karush-Kuhn-Tucker (KKT) equations (Kuhn and Tucker, 1951). The KKT equations are necessary conditions for optimality for a constrained optimization problem. If the problem is a so-called convex programming problem, that is, f(x) and $G_i(x)$, i = 1, ..., m, are convex functions; then, the KKT equations are both necessary and sufficient for a global solution point. Let x* be a local extremum point of function f subject to the constraints mentioned in Equations (5), (6) and (7). The Karush-Kuhn-Tucker equations can be stated as:

$$\mathbf{\nabla f(x^*) + \sum_{i=1}^{m} \lambda_i \,.\, \nabla\, G_i(x^*) = 0} \tag{8}$$

$$\mathbf{\lambda_i \,.\, \nabla G_i(x^*) = 0,\ i = 1, \dots, m_{\,e}} \tag{9}$$

$$\mathbf{\lambda_i \geq 0,\ i = m_e + 1, \dots m,} \tag{10}$$

In addition to the original constraints mentioned for function $f(\mathbf{x})$, the first equation describes a cancellation of the gradients between the objective function and the active constraints at the solution point. For the gradients to be canceled, Lagrange multipliers (λ_i, i = 1, ... , m) are necessary to balance the deviations in magnitude of the objective function and constraint gradients. Because only active constraints are included in this canceling operation, constraints that are not active must not be included in this operation and so are given Lagrange multipliers equal to 0. This is stated implicitly in the last two Karush-Kuhn-Tucker equations.

The solution of the KKT equations forms the basis to many nonlinear programming algorithms. These algorithms attempt to compute the Lagrange multipliers directly. Constrained quasi-Newton methods insure super linear convergence by accumulating the second-order information regarding the KKT equations using a quasi-Newton updating procedure. These methods are commonly mentioned as Sequential Quadratic Programming (SQP) methods, since a QP subproblem is solved at each major iteration, also known as Iterative Quadratic Programming (Hock and Schittkowski, 1983), Recursive Quadratic Programming (Biggs, 1973), and Constrained Variable Metric methods (Powell, 1983).

2.2.3 Sequential Quadratic Programming (SQP)

SQP methods represent the state of the art in nonlinear programming methods (Schittkowski, 1986). The method allows us to closely mimic Newton's method for constrained optimization just as is done for unconstrained optimization (Biggs, 1973; Han, 1977; Powell, 1978a, 1978b). At each major iteration, an approximation is made of the Hessian of the Lagrangian function using a quasi-Newton updating method which is then used to insure a QP subproblem whose solution forms a search direction for a line search procedure. A general review of SQP is found in -Fletcher, 2013; Gill et al., 1981; Powell, 1983; Schittkowski, 1986.

Given the problem description in GP (Equation 4), the principal idea is the formulation of a QP subproblem based on a quadratic approximation of the Lagrangian function.

$$\mathbf{L}(\mathbf{x},\boldsymbol{\lambda}) = \mathbf{f}(\mathbf{x}) + \sum_{\mathbf{i=1}}^{\mathbf{m}} \boldsymbol{\lambda}_{\mathbf{i}} \cdot \mathbf{G}_{\mathbf{i}}(\mathbf{x}). \qquad (11)$$

If x* is a local extremum point of the objective function f, then Equation (11) can be used in the procedure of the minimization in the following cases:

a) The constraint $\mathbf{G_i(x) = 0,\ i = 1, \dots, m}$. Assume that x* is a regular point of these constraints. Then, there is a $\boldsymbol{\lambda} \,\boldsymbol{\epsilon} \boldsymbol{R}^{\boldsymbol{m}}$ such that Equation (8) is satisfied, subject to the constraint.

b) If $m_e < m$, a constraint $G_i(\mathbf{x})$ is active at x* if $G_i(x^*) = 0$, and it is inactive if $G_i(x^*) < 0$. Note that all equality constraints are active.

c) If x* is a local extremum point of function f subject to Equation (5) and (6). Assume that x* is a regular point of these constraints. Then Equation (8), (9) and (10) are held.

The QP subproblem obtained by linearizing the nonlinear constraints. This subproblem can be solved using any QP algorithm. The solution of QP algorithm is used to form a new iterate

$$\mathbf{x_{k+1} = x_k + \boldsymbol{\alpha}_k d_k} \qquad (12)$$

The step length parameter α_k is determined by an appropriate line search procedure so that a sufficient decrease in a merit function is obtained and X_k and d_k are estimated by QP algorithm.

A nonlinearly constrained problem can often be solved in less iteration than an unconstrained problem using SQP. The reason for this is that, because of limits on the feasible area, the optimizer can make informed decisions regarding directions of search and step length. The process of nonlinear optimization that explained above is summarized and shown in Figure 1.

For implementation of the above-mentioned method for the inversion, a Matlab toolbox algorithm, named optimization tools, constrained nonlinear minimization, has been used.

2.3. Choosing Form of the Objective Function

This method has flexibility of using different forms of the objective function. For over-determined problem where the number of data is greater than that of model parameters and the inverse problem well-constrained by data and noise that has less effect on the instability of the inversion, the objective function can be chosen in one of the following forms:

2.3.1. Over and Even Determined Inverse Problems

$$\mathbf{f(x) = mean} = \frac{\sum_{i=1}^{N}|d_i^o - d_i^p|}{N} = \frac{\sum_{i=1}^{N}|d_i^o - g_i(x)|}{N} \quad (13)$$

$$\mathbf{f(x) = RMS} = \sqrt{\frac{\sum_{i=1}^{N}(d_i^o - d_i^p)^2}{N}}. \quad (14)$$

where f(x) is the objective function, x is a vector of model parameters, $\mathbf{d_i^o}$ is observed data, $\mathbf{d_i^p}$ is predicted data, g(x) is the forward model vector, mean is error average value, RMS is standard deviation or Root Mean Square error and N is the number of data. Sometimes, both of the above equations can be used in the case where the number of data is the same as that of model parameters (even determined problems, practically is not usual).

2.3.2 Underdetermined inverse problems

Making stability in the inversion can be achieved by defining other forms for the objective function such as the following:

$$\mathbf{f(x)} = \left\|\mathbf{W_d}\left(\mathbf{d^o} - (\mathbf{g(x)})\right)\right\|^2 + \boldsymbol{\beta}^2\|\mathbf{W_m x}\|^2 \quad (15)$$

In the above equation, the first term shows a weighted measure of the predicted error and the second one shows the weighted length of the model parameters. In this equation, β is called damping factor and shows the weight of each term in minimization, x is vector of model parameters, W_m is a matrix which weights model parameters, W_d is a matrix which weights data that may be diagonal, d^o is vector of observed data, g(x) is predicted data vector and f(x) is the objective function.

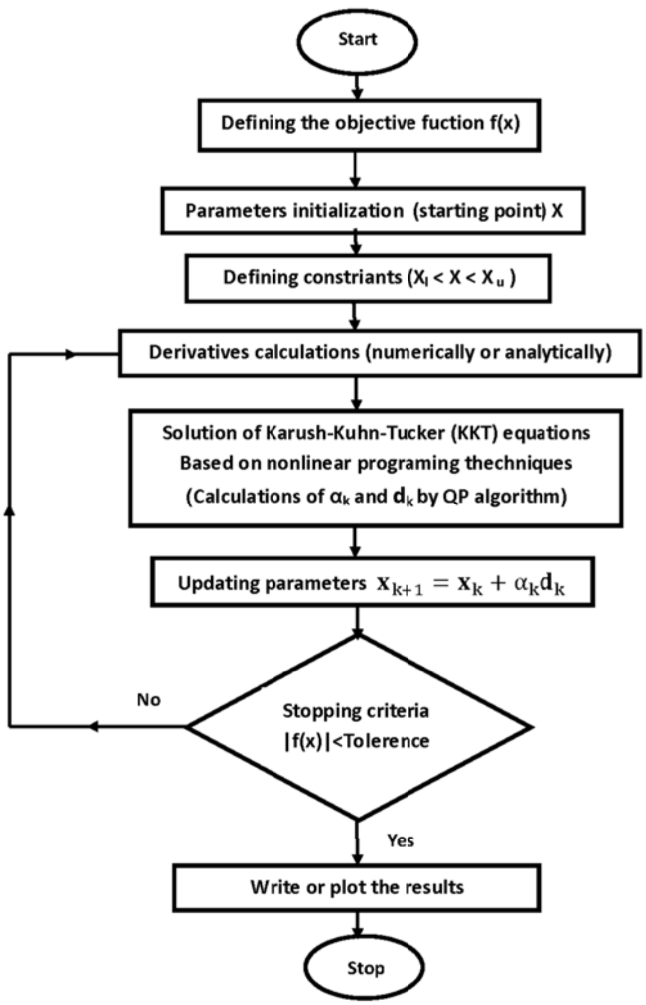

Figure 1. Flowchart of the non-linear constrained optimization algorithm.

When a small damping factor is chosen, most weight for minimization will be assigned to the first term (show unfitness between observed and calculated data) that may cause to an unreasonable model. However, when a large value is chosen for β, most weight will be assigned to the minimization of the second term (damping term), and this itself causes to a smooth model (without detail). Use of the second term called damping term causes the inverse problem be more stable, and the results also physically be more reasonable. Using the second term or damping term limits the searching space of model parameters and reduces under-determinacy part of the inverse problem. Despite these, the inverse problem becomes more resistant against the noise. Of course, there is a variety of manners for selecting β coefficient of the damping term or even different forms for the second term.

3. Inversion by Synthetic Data

3.1. Selective Synthetic Model

In order to specify the advantages and weaknesses of the method, as it is prevalent, the methodology should be examined by an obtained synthetic data of a theoretical model. For this reason, a relatively complex 2-D model has been designed. Assume that a sedimentary basin consisting of homogeneous sediments and basement can be modeled by a set of the elementary sources. A finite region of the x-z plan, containing entirely the basin, is discretized into M juxtaposed, 2-D prisms whose tops are at the earth's surface. The thicknesses of the prisms are the parameters to be estimated from the gravity data. Besides, for simplicity, the density contrast between the sediments and the basement is assumed to be kept constant and known. The only parameters to be estimated (thicknesses of elementary prisms) are related to the gravity field by the nonlinear relationship (Equation 2 or 3). The considered synthetic model (Figure 2.a) is formed by 40 elementary prisms, which approximate a sedimentary basin whose density contrast with the basement is considered constant (-0.5 g/cm^3). The model length is 30 km and the maximum depth of the sedimentary basin or depth of the basement is considered 4.5 km. The gravity effect of this synthetic model is calculated using Equation (3) and depicted in Figure 2.b.

As it can be seen in Figure 2.b, the length of the survey data or profile is about 30 km, the number of data point is 110, and the distance between measured points is taken 0.3 km.

3.2. Inversion of Synthetic Gravity Data

The synthetic data has been inverted using the nonlinear constrained inversion algorithm. The dependency of the objective functions on model parameters (here are depth of 2-D elementary prisms) is a nonlinear one. Since the problem is nonlinear, it needs some iteration to optimize initial defined model parameters.

To begin the inversion, it is needed to define an initial model composed of some model parameters. In this case, the number of model parameters selected are equal to those used for constructing synthetic model, meaning 40. Thus, in this case, the initial model was constructed from 40 prisms whose tops were selected at the surface and bottoms at depth 2 km. It means that the initial model was a flat model at depth 2 km. Lower and upper bounds considered for the inversion were 0 and 5 km, as the constraints for the model parameters during the procedure of the optimization. These were the only constraints used for the inversion.

In this section, we want to examine the effect of the noisy data on the inversion result. To do this, some Gaussian noise (about 5%) was added to the data so that the standard deviation error was about 2.4 mGal.

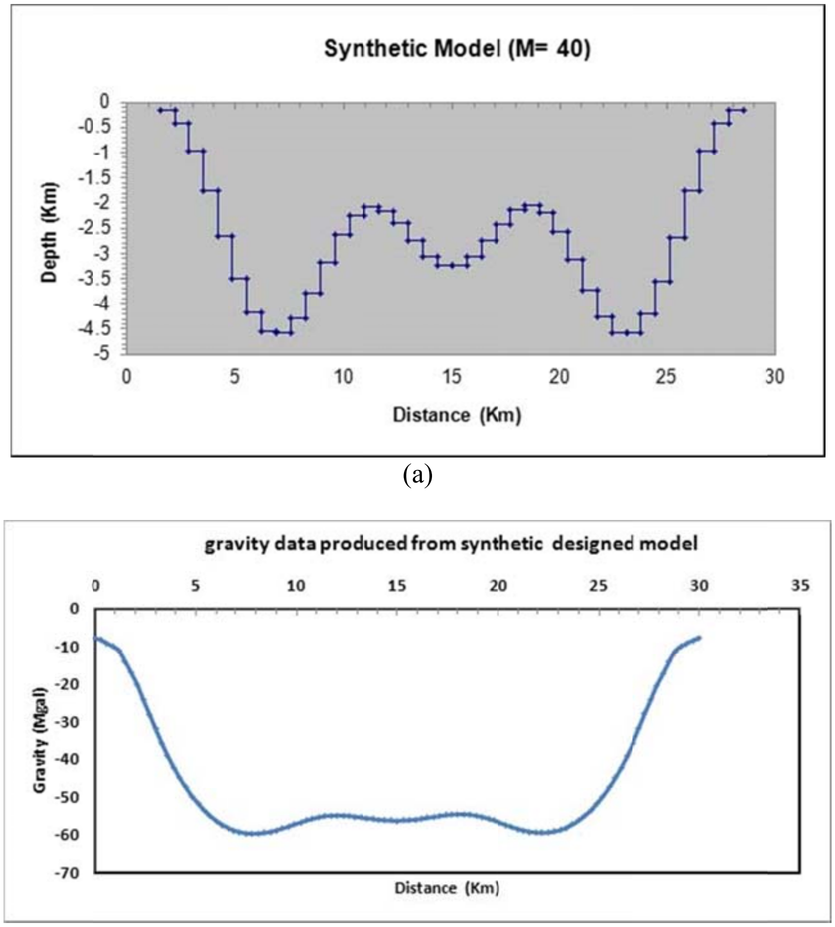

(a)

(b)

Figure 2. Designed synthetic model composed of 40 elementary prisms whose bottoms make interface between basement and sediments (a). Gravity response of the synthetic model (b).

In order to have better criteria for stopping iterations of the inversion, the objective function is defined in the form of standard deviation or Root Mean Square error as defined in Equation (14). The results of the inversion are shown in Figure 3.

In procedure of the inversion, the initial value of standard deviation was about 8 mGal that after 9 iterations reached less than 2.4 mGal. The convergent rate of the inversion was also rather fast, because just after 9 iterations, the objective function reached below the minimum value. Looking at in (Figure 3.a), it is observed that the inverted model is really similar to the original model (Figure 2), and there is also no instability in the model (even in the borders). Comparison of the gravity model response with that of the synthetic noisy data is shown in (Figure 3.b); the effect of the Gaussian noise in the form of undulations can also be seen on the figure.

As shown, there is a good adjustment between the gravity response of the model and the part of free-noise observed data. This means that the noise has roughly less role in the optimization, and the original model that has been reproduced with a good approximation. As a result, it can be said that the applied method used for the inversion is relatively resistant against the noise, as if the effect of noise is not so tangible in the inverted model.

4. Real Gravity Data Inversion

4.1. Geology Setting

The sediment basin of Aman Abad area is located in south part of desert Mighan (Figure 4). In this region, the highest place is assigned to the mountain of Haftad Gholeh with a height about 2720 m and the lowest one to Lake of Mighan desert about 1660 m.

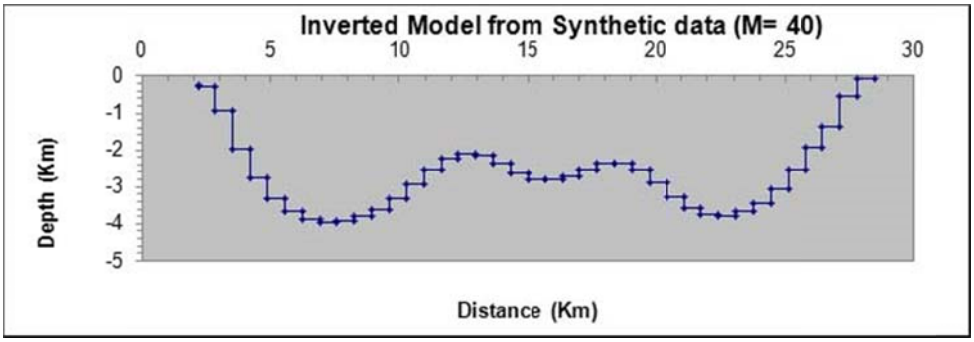

(a)

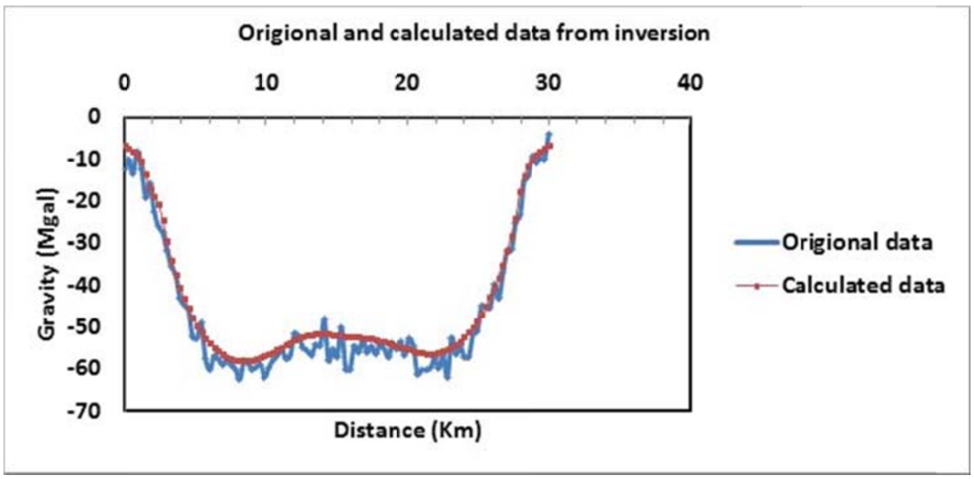

(b)

Figure 3. Result of the inversion of synthetic noisy gravity data (a), comparison of the observed and calculated gravity data (b).

According to the geological and classification of Iran, a major part of the Aman Abad area is located in the Sanandaj-Sirjan zone, and a partial part of it is also located in subzone of Haftad Gholeh. The Tabateh and Talkhab, big faults in this area, have general northwest - southeast trend that is the same as that of Zagros main trend.

Most of the sedimentary of this area includes limy slate in Cretaceous period. Some of the intrusion formations which made granodiorite rocks in this area have also penetrated in these limes. The movement of Laramide Orogeny has caused some folds, transformation, upductions and magma intrusions. In the effect of this movement, limes of Cretaceous period have been shaped in slate form. In addition to the faults, there are many fractures with seams and cavities in the formations that provide the main resource of the underground water for Arak plain.

4.2. Modeling of the data

The proposed method was applied to the gravity anomaly of Aman Abad basin to determine the relief of interface separating two homogeneous media, sediments and basement. The same as synthetic case, upper medium is discretized into rectangular, juxtaposed prisms whose thicknesses represent the depths to the interface and are the parameters to be estimated from the gravity anomaly data inversion. The density contrasts of all prisms are assumed to be constant and known.

As gravity anomaly has some components influenced by the regional trend, regional anomaly has also been determined and removed from the measured data.

The survey of real gravity data in Aman Abad area has been done by gravimeter of type CG3, SCINTREX, (automated gravimeter of Institute of Geophysics of University of Tehran), along six profiles A, B, C, D, E and F orienting western-eastern. The accuracy of the gravimeter is about 0.005 mGal and fortunately, this device itself, does tidal correction automatically. The number of total data is 259, which are distributed on the profiles. In Figure 5, the position of profiles is shown on topography contours map of the area.

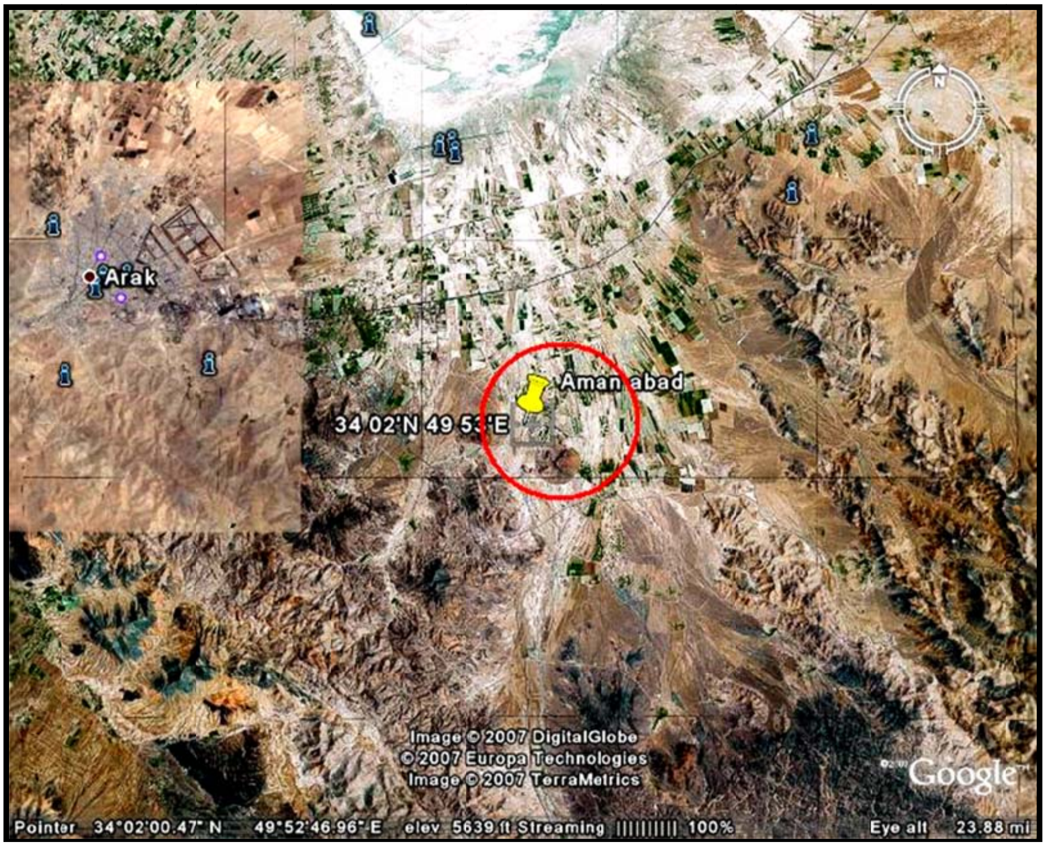

Figure 4. The position of the studying area by Google Earth.

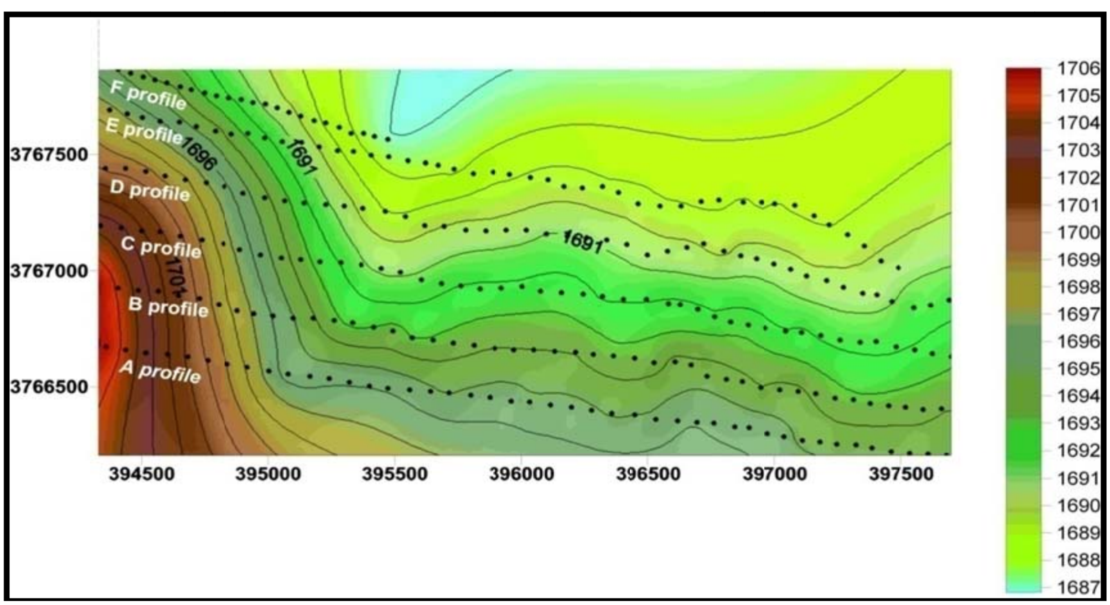

Figure 5. Position of the gravity profiles on the topography contours map.

The distance between measurement points is about 60-80 m, the distance between profiles is about 250 m, and total area of the survey zone is about 5 km^2.

In order to get gravity anomaly data for the inversion, different corrections have been performed on the raw data and the trend is calculated and reduced from the corrected data.

By fitting the observed data with orthogonal and orthonormal polynomials that are independent functions, the regional trend effect of the data was calculated.

Then, residual data were obtained by reducing the calculated regional effect from the observed data (Sarma et al, 1990).

The cause of using mentioned polynomials rather than ordinary ones is that a set of linear equations formed from them that will not be ill-conditioned, and convergence rate of this method is more than the least squares approximation techniques. Thus, using this method for calculating trend coefficients will be more efficient than the ordinary least squares techniques (Sarma et al, 1990). Selecting the number and order of these polynomials for calculating regional effect was formed by using the F test statistical analysis (Sarma et al, 1990). Concerning the mentioned statistical analysis, polynomials of order 3 were considered for calculating the effect of the regional trend. Calculated 2-D Bouguer gravity anomaly (residuals) map of the area has been depicted in Figure 6.

Due to lack of the space here, only data inversion results of some selected profiles will be presented in the following.

4.2.1. Inversion of Gravity Data from Profile A

There are about 41 survey data on this profile, oriented east-western. For inversion of this gravity anomaly data, as the number of data is rather low, three types of parameterizations have been made:

1) Over-determined, 2) Even-determined, 3) Under-determined

1) Over-determined

Here, a model consisting of 15 prisms that their upper height show horizontal surface and their lower height show the interface between sedimentary and bedrock, have been considered. The positions of some drinking water wells in this area are shown in Figure 7. Excavated depths of these wells are different. They have been excavated as far as they fulfill the need for water and some of them reach the bedrock. Sediments thickness of wells number 4 and 15, which have reached the bedrock are about 140 m. Depth of other wells are about 100 m and have not excavated to the bedrock depth yet.

From information of the dug wells in this area, the maximum depth of the sediments or maximum depth of the bedrock was considered to be about 200 m for doing all real data inversions. Thus, the average depth of the sediments for all inversions was considered about 100 m. Based on this information, the upper and lower bound for sediments thickness for the inversions have been considered 0 and 200 m. For this case, model parameterization was performed in a way that the number of data is greater than those of model parameters (over-determined). The objective function considered for this case was that of defined in Equation (14). The density contrast between bedrock and sediments was obtained based on some gathered downhole data in this region. The lithologic descriptions of well number 4 and 15 are shown in Table 1. In the table, observed lithology intervals for each borehole are indicated. The lithology materials of the sediment intervals are composed of clay, sand, gravel and cobble, with different percentage at different depths. As mentioned in the table, bedrock material is schist. Density contrast between the sediments and the bedrock was estimated about 0.5 g/cm^3. This was considered constant during the optimization procedure and only lower depths of the prisms have been changed. The result of this inversion is shown in Figure 8.

Decreasing rate of the objective function was fast, after 15 iterations, its value reached 0.019967 mGal. The depth of the sedimentary basin increases from west to east, and in the center, it reaches the maximum (about 200 m), including also an uplift (Figure 8.a). The gravity response of the inverted model and observed data are depicted in Figure 8.b. As shown, the agreement between two data sets is reasonable except in the east, due to the side effect and result of incomplete survey data along this profile.

2) Even-determined
Profile A
To examine the efficiency of the method, a finer parameterization was considered for the model. In this case, the considered model approximated by 40 rectangular prisms whose lower depths shape the geometry of the basement along this profile.

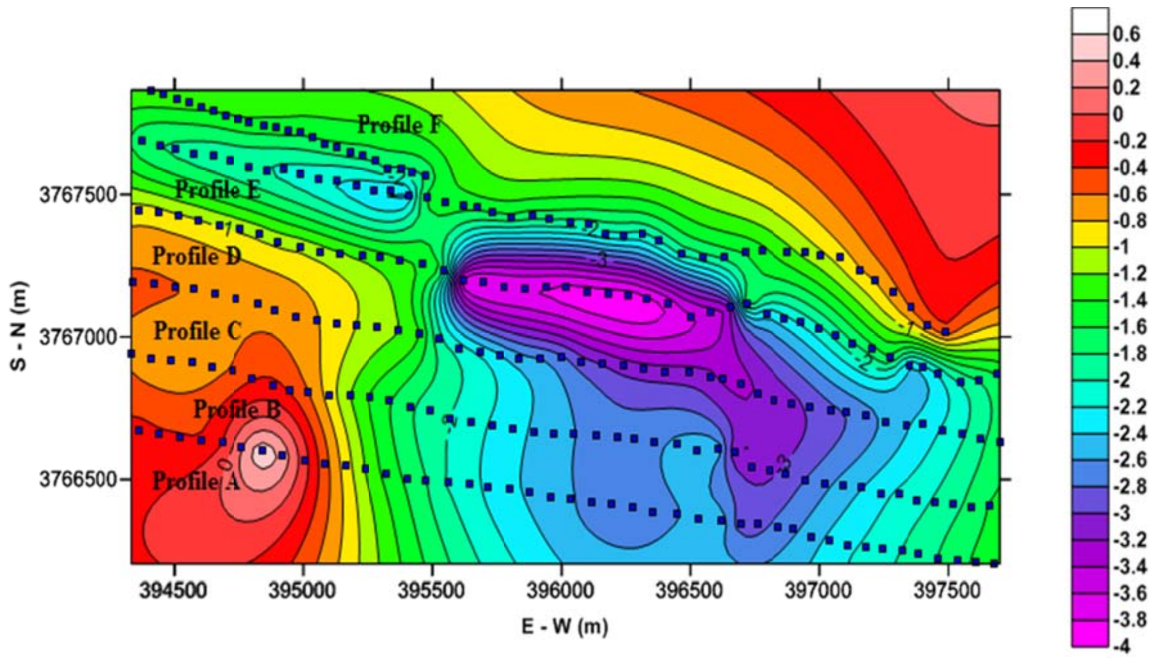

Figure 6. 2-D Bouguer gravity anomaly (mGal) together with the position of the stations and the profiles.

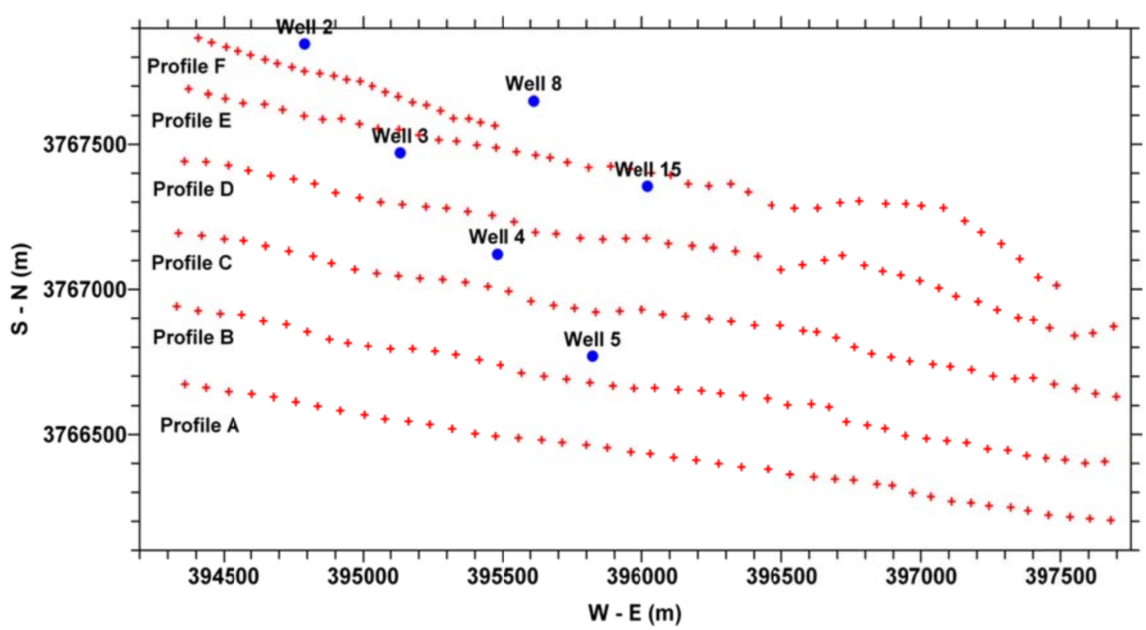

Figure7. Positions of excavated drinking water wells on the measured gravity data profiles map.

Table 1. Lithology types tables of well number 4 and 15 from the gathered downhole data.

Lithology of well number 4			
Interval number	Materials name	Materials percentage	Interval depth(m)
1	Soil	100	0-5
2	Clay- Gravel - Sand	50 – 30 -20	5-30
3	Clay- Gravel -Sand- Cobble	30 – 30 -20 -20	30 - 80
4	Clay- Gravel -Sand- Cobble	25 – 25 – 25 - 25	80 -110
5	Clay- Gravel -Sand	50 -30 - 20	110 -120
6	Marl	100	120 -140
7	Schist		140
Lithology of well number 15			
Interval number	Materials name	Materials percentage	Interval depth (m)
1	Soil	100	0-5
2	Clay- Gravel -Sand	30 -35 - 35	5-30
3	Clay- Gravel -Sand	50 – 25 -25	30 - 50
4	Clay- Gravel -Sand- Cobble	35 – 20 – 20 - 25	50 -90
5	Clay- Gravel -Sand- Cobble	40 -20 – 20 - 20	90 -115
6	Clay- Gravel -Sand- Cobble	60 -15 – 15 - 10	115 -130
7	Schist		130

By selecting this parameterization, inverse problem becomes underdetermined. This may make some instability in the model during the process of the optimization. The inversion result using the mentioned objective function (Equation (14)) is shown in Figure 9.

The decreasing rate of the objective function was also fast, after 40 iterations its value reached 0.0022436 mGal. The geometry of the bedrock shows an unreasonable geology feature, especially in the east (right side) that indicates some instability in the model (Figure 9.a).

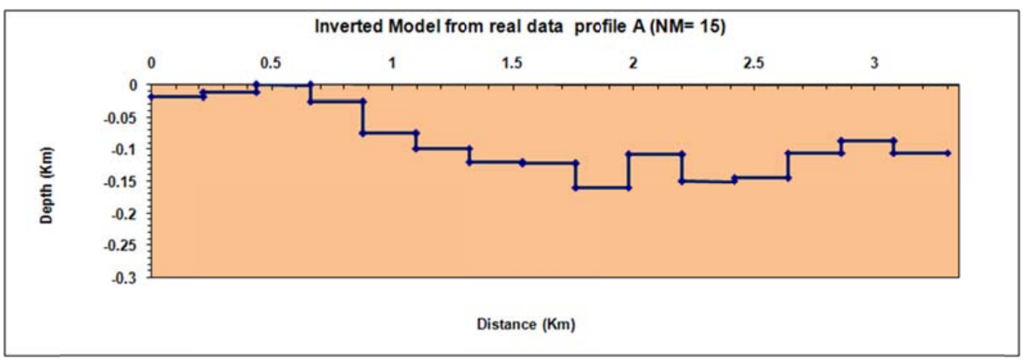

(a)

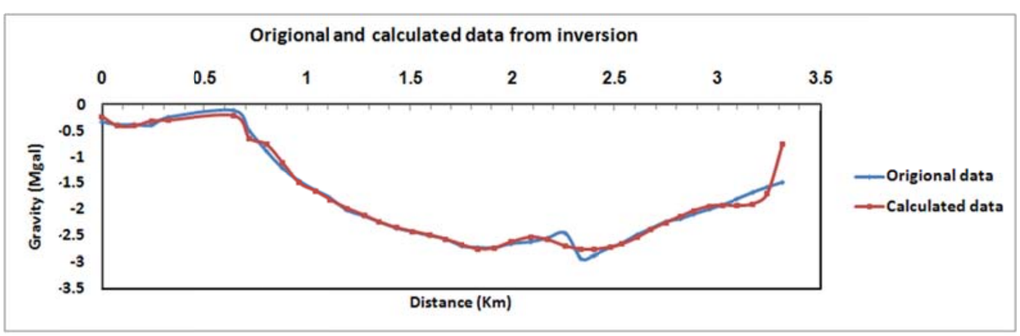

(b)

Figure 8. Produced model (15 model parameters) from the inversion (a) and gravity response of the inverted model together with the real gravity data (b), along profile A.

Although the agreement between gravity response of the inverted model and the observed data is good (Figure 9.b), due to the existence of inherent non-uniqueness of inverse problems, the resulted unstable model is not often reliable in geological sense.

Profile B

Now, for making stability in the inversion, a new objective function that consists of two terms was used: first, the minimization of error vector length of data; second, the minimization of the model parameters vector length that can be defined with variety forms (Equation 15).

As mentioned before, there is a variety of manners for selecting β. Here, the value 0.2 is assigned to the damping coefficient β, for the inversion. Results of the inversion are shown in Figure 10.

The minimization rate of the objective function was rather fast, and after 40 iterations, its value decreased to 0.85115.

As shown, we could control the previous instability and produce a model that is geologically reasonable. Uplift in the central part of the model can be seen; however, the observed instabilities have been eliminated and any unexpected undulation in this model is not observable. There is a good agreement between the gravity model response and measured data. The partial unfitting in central part may be because of existing noise or due to the smoothness or damping.

3) Under-determined

To show that the defined objective function is consisted of two terms (Equation 15) which can handle underdetermined inverse problems, the data of profile A, when the number of data is less than that of model parameters (under-determined problem), was also inversed.

For this case, this time, the model is constructed of 60 parameters and the same previous 41 data. As before, the initial model which was chosen a flat one at depth 100 m had changed between 0 and 200 m during the optimization procedure. For this case, damping coefficient β, was assigned 0.2. The result of this inversion is shown in Figure 11.

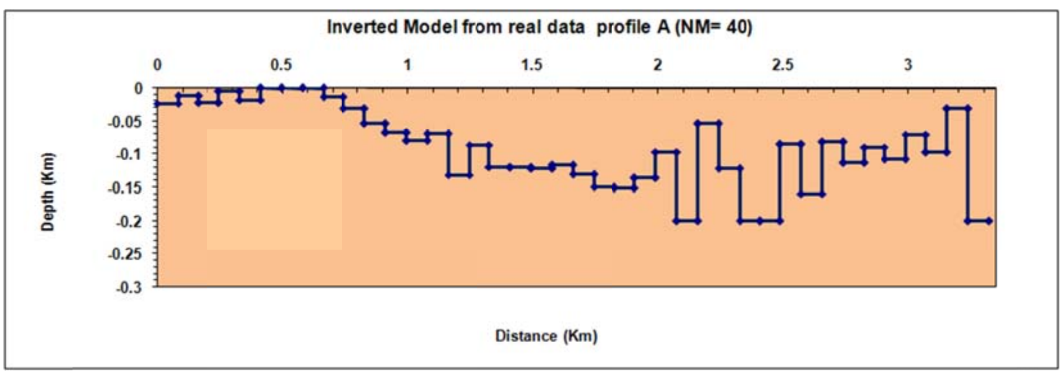

(a)

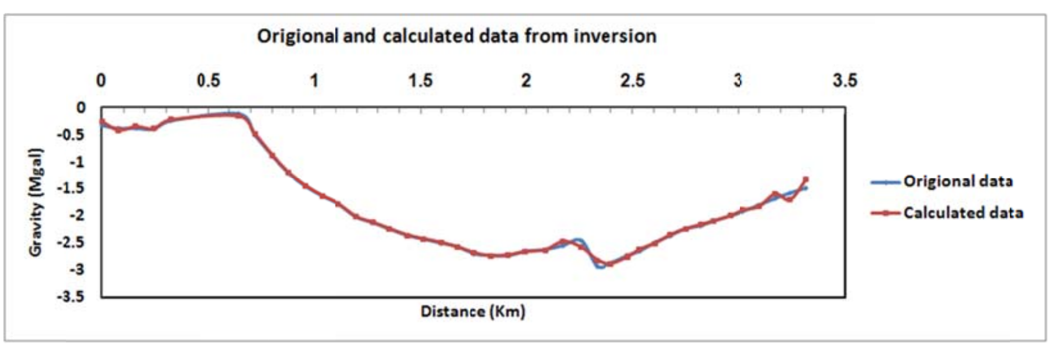

(b)

Figure 9. Produced model (40 model parameters) from the inversion (a) and gravity response of the inverted model together with the real gravity data (b), along profile A.

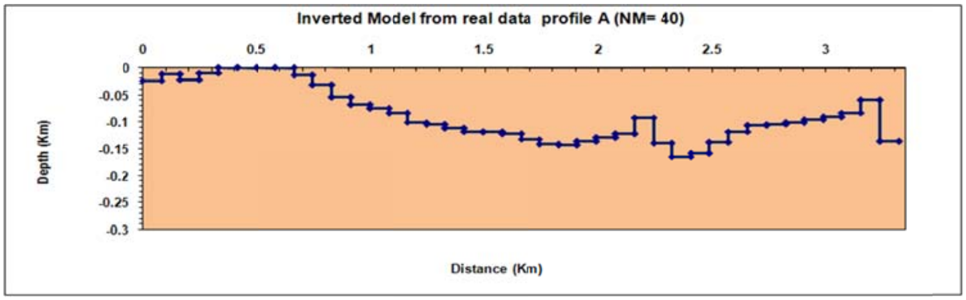

(a)

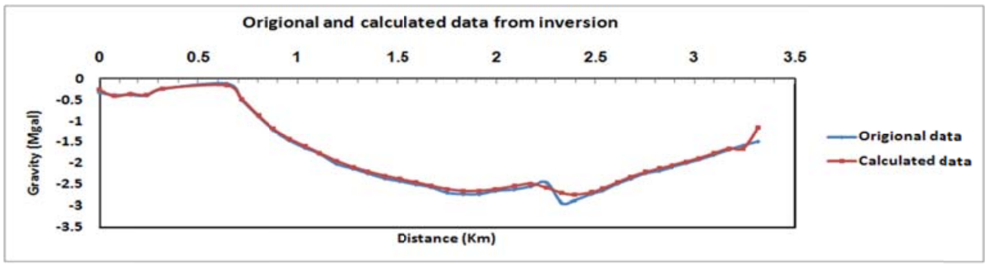

(b)

Figure 10. Produced model (40 model parameters) from the inversion using damping term (a), and gravity response of the inverted model together with the real gravity data (b), along profile A.

The decreasing rate of the objective function was rather fast, and after 60 iterations, its value has reached 0.1236. As shown in Figure 11.a, the geometry of sedimentary basin is almost like the previous ones, except in the east side. There is a rational adjustment between the gravity response produced of this model and the observed data, as shown in Figure 11.b.

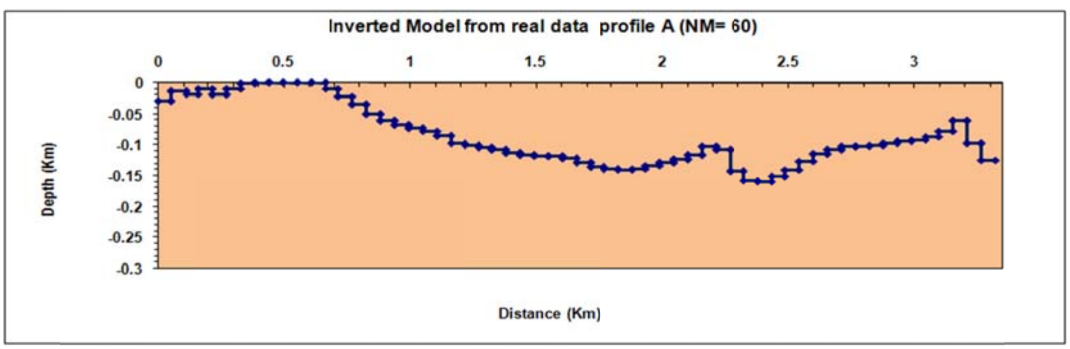

(a)

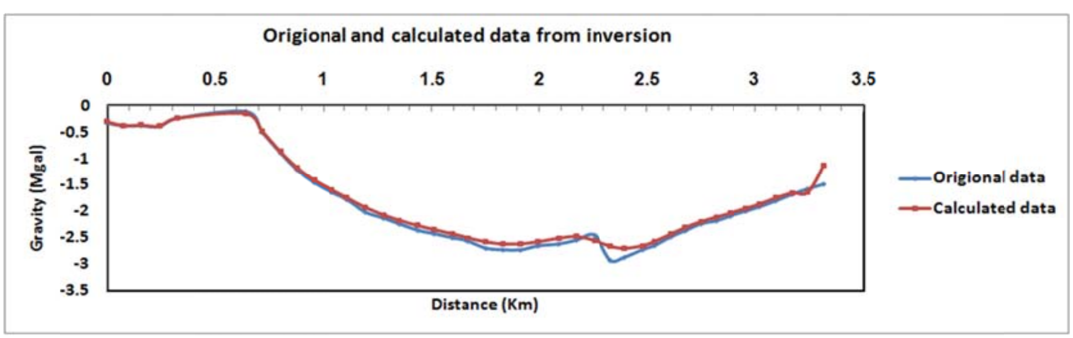

(b)

Figure 11. Produced model (60 model parameters) from the inversion using damping term (a), and the gravity response of the inverted model together with the real one data (b), along profile A.

It should be noted that, in the under-determined cases, each model parameter is estimated as a combination of its neighboring parameters. This is the nature of this kind of inverse problems. By doing this inversion, it has been shown that this method would be suitable for both the over and under-determined cases.

4.2.2 Inversion of Gravity Data from Profile C

Collected data along this profile has almost a west – east direction that roughly pass through the center of the anomaly (Figure 6). The number of data along this profile is 45, with maximum anomaly of about 3.5 mGal. Inversion of this data was implemented by choosing an initial flat model at the depth of 100 m, consisting of 20 parameters. This parameterization was chosen to take advantage of the over-determined condition for the inverse problem. It is clear that choosing this model parameterization did not need to use the objective function that consists of damping term. Thus, optimization procedure was performed using a simple objective function such as Equation (14). Results of this inversion are shown in Figure 12.

The decreasing trend of the objective function was fast, after 20 iterations its value reached 0.0075562. The maximum depth of the sediments is about 200 m (Fig. 12.a).

To investigate the dependency of the inversion results on choosing different initial models, in this case, the inversion was also implemented by considering an initial model at depth 1000 m. The used initial model was not only chosen outside the defined bounds (0 - 200 m), but also chosen 10 times greater than the considered average depth (100 m). The model from this inversion is also shown together with the model from the previous inversion (Figure 12.a). Gravity response of these two models is also depicted with corresponding observed gravity data in Figure 12.b. As can be seen in the figures, the two models and two data sets from the two inversions have a good agreement with each other. This fact could be shown for all inversions; however, due to the lack of the space here, only one of them is presented. Results of this investigation show that the inversion method is less dependent on choosing the initial model in a reasonable range.

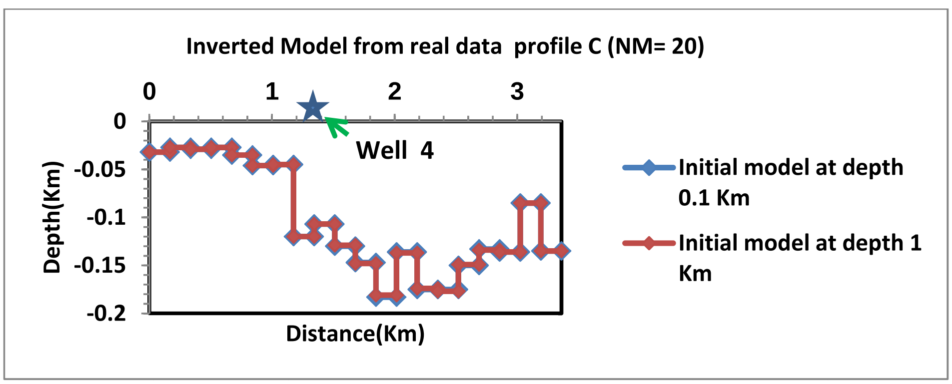

(a)

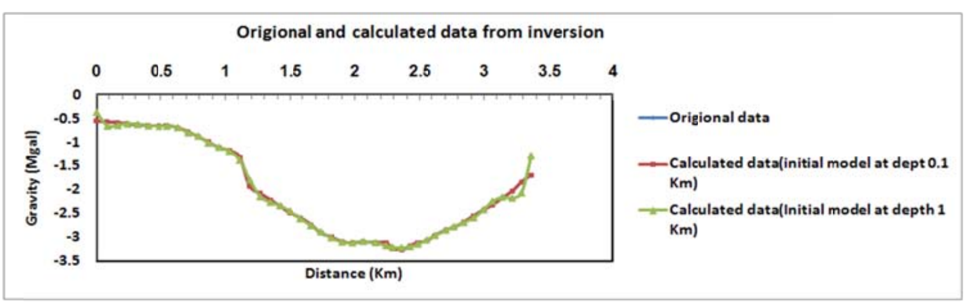

(b)

Figure 12. Produced model (20 model parameters) from the inversion (a), and the gravity response of the inverted model together with the real one data (b), along profile C.

In this figure, observed sudden variations in depths of the interface in the model can be interpreted as fault, such as in horizontal positions about 1.2 km. In this inversion, the number of the data was about three times of that of the model parameters. In this way, a good constraint is implemented on the inversion by data. Thus, the resultant model is reliable and any instability cannot be seen in the model. As shown in Figure 12.b, a good fit is observable between gravity responses of the model with the measured data along this profile.

The nearest well to this profile is well number 4 whose approximate position is shown on the profile (Figure 12.a). As it can be seen, at this position, the thickness of the sediments from the inverted model is about 120 m, which is roughly less than the depth of the well which is 140m (Table 1). The cause of the difference is that the thickness of sediments to the north direction and to the anomaly center should increase (see Figure 6).

It is necessary to mention that the results of the inversions from other data profiles and different parameterization, such as those used for data profile of A and C are not shown here due to the lack of the space.

5. Conclusions

In this study, a 2-D model composed of a set of juxtaposed prisms whose lower faces were considered as unknown model parameters that approximated the geometry of a basement. Synthetic and real gravity data were inverted using a nonlinear inversion technique and an optimization procedure. Density contrast between sediments and basement was taken known for the inversion.

Results of the inversion of both synthetic and real data showed that this method has a noticeable efficiency and flexibility in inverting data. The results also show that this method is able to map the geometry of sedimentary basins, detecting features such as uplifts and faults, using inverting gravity data, which have many practical applications in the earth science branches. Delineating the thickness of the sediments in the basin is also one of the key factors for exploring water potentials in the area and detecting fractures.

Finally, it should be mentioned that each inversion method has its advantages and weaknesses that depend on for what geophysical problem in hands is used. The method used here for solving a practical problem in gravity, means estimating geometry of basin interface from the measured gravity data, that maybe approached using other nonlinear inversion techniques. Some of them are referred in the introduction part, but some advantages of using this method can be pointed out as follows:

a) There is flexibility on choosing the objective function for the inversion, in procedure of the nonlinear optimization (depending on the problem conditions).

b) Handling under-determined and over-determined inverse problems.

c) Using partial derivatives analytically (if possible) or numerically for the inversion.

d) Introducing different constraints for the inversion, in the form of upper or lower bounds or introducing them in the form of equations.

e) The inversion technique used is less dependent on choosing the initial model in a reasonable range.

f) Basic algorithm of nonlinear optimization is simple for programming and does not need to write a complicated program.

Acknowledgment

The authors would like to express their gratitude to Prof. Ebrahimzadeh Ardestani V., the head of Gravity Department in Institute of Geophysics of University of Tehran, who assisted in collecting the measured gravity data in Aman Abad area.

References

Abbott, R. E. and Louie, J. N., 2000, Depth to bedrock using gravimetry in the Reno and Carson City, Nevada, area basins. Geophysics, 65(2), 340-350.

Annecchione, M. A., Chouteau, M. and Keating, P., 2001, Gravity interpretation of bedrock topography: the case of the Oak Ridges Moraine, southern Ontario, Canada. Journal of Applied Geophysics, 47(1), 63-81.

Barbosa, V. C., Silva, J. B. and Medeiros, W. E., 1999, Gravity inversion of a discontinuous relief stabilized by weighted smoothness constraints on depth. Geophysics, 64(5), 1429-1437.

Bell, R. E., Childers, V. A., Arko, R. A., Blankenship, D. D. and Brozena, J. M., 1999, Airborne gravity and precise positioning for geologic applications. Journal of Geophysical Research: Solid Earth, 104(B7), 15281-15292.

Biggs, M., 1973, Constrained minimisation using recursive quadratic programming: some alternative subproblem formulations: Hatfield Polytechnic. Numerical Optimisation Centre.

Blakely, R. J., 1996, Potential theory in gravity and magnetic applications: Cambridge University Press.

Burkhard, N. and Jackson, D. D., 1976, Application of stabilized linear inverse theory to gravity data. Journal of Geophysical Research, 81(8), 1513-1518.

Chakravarthi, V. and Sundararajan, N., 2007, 3D gravity inversion of basement relief—A depth-dependent density approach. Geophysics, 72(2), I23-I32.

Courtillot, V., Ducruix, J. and Le Mouël, J. L., 1974, A solution of some inverse problems in geomagnetism and gravimetry. Journal of Geophysical Research, 79(32), 4933-4940.

Fletcher, R., 2013, Practical methods of optimization: John Wiley and Sons.

Gill, P. E., Murray, W. and Wright, M. H., 1981, Practical optimization.

Granser, H., 1987, Nonlinear inversion of gravity data using the Schmidt-Lichtenstein approach. Geophysics, 52(1), 88-93.

Guspi, F., 1993, Noniterative nonlinear gravity inversion. Geophysics, 58(7), 935-940.

Han, S.-P., 1977, A globally convergent method for nonlinear programming. Journal of Optimization Theory and Applications, 22(3), 297-309.

Hock, W. and Schittkowski, K., 1983, A comparative performance evaluation of 27 nonlinear programming codes. Computing, 30(4), 335-358.

Kuhn, H. W. and Tucker, A. W., 1951, Nonlinear programming. Paper presented at the 2nd Berkeley Symposium. Berkeley, University of California Press.

Li, X., 2010, Efficient 3D gravity and magnetic modeling. Paper presented at the EGM 2010 International Workshop.

Oldenburg, D. and Pratt, D., 2002, Geophysical inversion for mineral exploration. Geophysical Inversion Facility, 1-53.

Parker, R., 1973, The rapid calculation of potential anomalies. Geophysical Journal International, 31(4), 447-455.

Pedersen, L. B., 1977, Interpretation of Potential Field Data a Generalized Inverse APPROACH*. Geophysical Prospecting, 25(2), 199-230.

Pilkington, M., 2006, Joint inversion of gravity and magnetic data for two-layer models. Geophysics, 71(3), L35-L42.

Pilkington, M. and Crossley, D., 1986, Determination of crustal interface topography from potential fields. Geophysics, 51(6), 1277-1284.

Plouff, D., 1966, Digital terrain corrections based on geographic coordinates. Paper presented at the Geophysics.

Powell, M., 1983, Variable metric methods for constrained optimization Mathematical Programming, The State of the Art, 288-311, Springer.

Powell, M. J., 1978a, The convergence of variable metric methods for non-linearly constrained optimization calculations. Nonlinear Programming, 3.

Powell, M. J., 1978b, A fast algorithm for nonlinearly constrained optimization calculations Numerical analysis, 144-157, Springer.

Richardson, R. M. and MacInnes, S. C., 1989, The inversion of gravity data into three-dimensional polyhedral models. Journal of Geophysical Research: Solid Earth, 94(B6), 7555-7562.

Sarma D. D. and Selvaraj J. B., 1990, Two dimensional orthonormal trend surfaces for processing. Computer and Geosciences, 16(7), 897-909.

Schaefer, D. H., 1983, Gravity survey of Dixie Valley, west-central Nevada: US Geological Survey.

Schittkowski, K., 1986, NLPQL: A FORTRAN subroutine solving constrained nonlinear programming problems. Annals of Operations Research, 5(2), 485-500.

Silva, J. B., Oliveira, A. S. and Barbosa, V. C., 2010, Gravity inversion of 2D basement relief using entropic regularization. Geophysics, 75(3), I29-I35.

Smith, R. A., 1961, A uniqueness theorem concerning gravity fields. Paper presented at the Mathematical Proceedings of the Cambridge Philosophical Society.

Studinger, M., Bell, R. E., Blankenship, D. D., Finn, C. A., Arko, R. A., Morse, D. L., and Joughin, I., 2001, Subglacial sediments: a regional geological template for ice flow in West Antarctica. Geophysical Research Letters, 28(18), 3493-3496.

Zhou, X., 2013, Gravity inversion of 2D bedrock topography for heterogeneous sedimentary basins based on line integral and maximum difference reduction methods. Geophysical Prospecting, 61(1), 220-234.